Molecular dynamics simulations of hydrated unsaturated lipid bilayers in the liquid-crystal phase and comparison to self-consistent field modeling

A. L. Rabinovich and P. O. Ripatti
Institute of Biology, Karelian Research Center, Russian Academy of Sciences, Pushkinskaja Street 11, Petrozavodsk, 185610, Russia

N. K. Balabaev
Institute of Mathematical Problems of Biology, Russian Academy of Sciences, Pushchino, Moscow Region 142292, Russia

F. A. M. Leermakers
Laboratory of Physical Chemistry and Colloid Science, Wageningen University, Dreijenplein 6, 6703 HB Wageningen, The Netherlands
(Received 29 December 2001; published 28 January 2003)

Molecular dynamics simulations, using the collision dynamics method, were carried out for hydrated bilayers of 1-stearoyl-2-oleoyl-*sn*-glycero-3-phosphatidylcholine (18:0/18:1ω9*cis* PC, SOPC) and 1-stearoyl-2-docosahexaenoyl-*sn*-glycero-3-phosphatidylcholine (18:0/22:6ω3*cis* PC, SDPC). The simulation cells of the two bilayers consisted of 96 SOPC (or SDPC) molecules and 2304 water molecules: 48 lipid molecules per layer and 24 H_2O molecules per lipid. The water was modeled by explicit TIP3P water molecules. The C—H bond-order-parameter $-S_{CH}$ profiles of the hydrocarbon tails, the bond orientation distribution functions and the root-mean-square values of the positional fluctuations of the lipid chain carbons were calculated. Simulation results are compared to the available experimental data and to other computer investigations of these lipid molecules. Several results of molecular-level self-consistent field calculations of these bilayers are also presented. Both theoretical methods reveal the same main characteristic features of the order-parameter profiles for the given bilayers. Some aspects of the physical properties of unsaturated lipids and their biological significance are discussed.

DOI: 10.1103/PhysRevE.67.011909 PACS number(s): 87.16.Dg, 87.14.Cc, 81.16.Dn, 31.15.Qg

I. INTRODUCTION

A large number of cellular processes is associated with biological membranes [1]. Membranes are constructed of bilayers of lipid molecules, they include in addition an array of proteins and other molecular components. Lipids are a chemically diverse group of compounds; they play an important role in cell structure and function. Lipids may contain a wide variety of hydrocarbon (for the most part, unbranched) chains of fatty acids; the most commonly occurring chains have 12–24 carbons. These chains may contain one or more (up to six) carbon-carbon double bonds (as a rule, of the *cis* configuration) in different positions. In most monounsaturated fatty acid chains, the double bond is between the ninth and tenth carbons (the first one being the carbonyl group carbon). The double bonds of polyunsaturated chains are, as a rule, separated by a methylene group, i.e., the double bonds are methylene interrupted. Below we will use the notation $N{:}k\omega j$ for the fatty acid chain structure, where N refers to the total number of carbon atoms in the chain, k is the number of (methylene-interrupted) double bonds and j denotes the number of carbons between the CH_3 group of the chain and the nearest double bond.

Biological membranes are complex in lipid composition, they demonstrate a relatively high degree of heterogeneity: a typical membrane contains many species of lipid molecules, with different head groups and hydrocarbon tails [1] and, in most cases, at least half of the fatty acyl chains are unsaturated. The physical characteristics of unsaturated lipids are the central issues in the present work. Some animal and plant species, tissues, or organs may be cited which contain membranes with one or several unsaturated lipid chains as their main component. Monounsaturated fatty acid chains are the main component in some bacterial membranes [2]; linolenic acid (18:3ω3*cis*) chain is the major acyl constituent of lipids of higher plant chloroplasts [3,4]; docosahexaenoic acid (22:6ω3*cis*) chain is important in maintaining the normal structure and function of the retina [5,6], and 22:6ω3*cis* makes up about half of the total fatty acids of vertebrate rod outer segment phospholipids, e.g., 35 to 60% of the fatty acids of phosphatidylethanolamine (PE) and phosphatidylserine (PS) in the photoreceptor outer segments in frogs and humans. A high content of ω3 highly unsaturated fatty acids, especially 22:6ω3*cis*, is a feature of the central nervous system [7,8]. The chains of 20:4ω6*cis*, 22:5ω3*cis*, and 22:6ω3*cis* are efficiently taken up and actively esterified into the lipids of mammalian brain [9,10]. Docosahexaenoic acid chain comprises approximately one-third of the fatty acid content of PE and PS in the cerebral cortex of humans, monkeys, and rats [8]. 22:6ω3*cis*-containing phospholipid species are constituents of spermatozoa [11]. It has been observed that membranes that are active metabolically, as in rod outer segments, mitochondria, sperm, and synaptic vesicles, have high levels of polyunsaturated fatty acid chains. It has been found as well that the content of 22:6ω3*cis* in both marine and freshwater fish is closely correlated with the level of fish species mobility [12]: the content is highest in highly active species.

There is an extensive literature about the fatty acid chain composition in relation to the roles of the *cis* double bonds in membranes [3,5,7,8,13–22]. Even though possible mechanisms of the effects of unsaturated fatty acid chains on the

membrane structure and dynamics can now be formulated, and much is known about the effects of lipid unsaturation on the physical properties of membranes, a full understanding of these processes at the molecular level is not yet achieved. Further experimental and theoretical investigations of the properties of various lipids, lipid monolayers, bilayers and other membrane systems are needed to provide additional information. Nuclear magnetic resonance [22–26], x-ray and neutron diffraction [26,27], fluorescence measurements [28–30], differential scanning calorimetry [31,32], micropipette pressurization [33] and other experimental techniques are modern tools to investigate different properties of hydrocarbon chains of unsaturated phospholipid bilayers.

A powerful and a subtle tool for studying different lipid molecules and lipid membrane systems is computer simulations of their realistic models. Molecular dynamics (MD), Monte Carlo, Langevin dynamics, Brownian dynamics methods are used (for recent reviews, see Refs. [34–37]). A computer simulation gives access to unprecedented detailed information on membrane systems, especially on the nanosecond time scale. As yet most simulations have been performed for saturated lipid systems, and comparatively few MD simulations have been carried out on unsaturated lipid systems. The objective of simulations is to obtain a molecular level understanding of structural as well as dynamical properties. Simulations on unsaturated lipids comprise 1-palmitoyl-2-oleoyl-*sn*-glycero-3-phosphatidylcholine (16:0/18:1ω9*cis* PC) bilayer-water system [38–40], 1-palmitoyl-2-elaidoyl-*sn*-glycero-3-phosphatidylcholine (16:0/18:1ω9*trans* PC) bilayer-water system [40], glycerol 1-monooleate (18:1ω9*cis* G) bilayer-water [41], dioleoylphosphatidylethanolamine (18:1ω9*cis*/18:1ω9*cis* PE) bilayer-water [42] and dioleoylphosphatidylcholine (18:1ω9*cis*/18:1ω9*cis* PC) bilayer-water systems [39,42–44], monolayers of diacylglycerolipids (DGs) that contained stearoyl (18:0) in the position *sn*-1 and oleoyl (18:1ω9*cis*), linoleoyl (18:2ω6*cis*), linolenoyl (18:3ω3*cis*) [45–49] or arachidonoyl (20:4ω6*cis*) and docosahexaenoyl (22:6ω3*cis*) [47–51] in the position *sn*-2, bilayers of the five above mentioned unsaturated DGs (18:0/18:1ω9*cis* DG, 18:0/18:2ω6*cis* DG, 18:0/18:3ω3*cis* DG, 18:0/20:4ω6*cis* DG, 18:0/22:6ω3*cis* DG) [52], 1-palmitoyl-2-linoleoyl-*sn*-glycero-3-phosphatidylcholine (16:0/18:2 ω6*cis* PC) bilayer-water system [53–55] and 1-stearoyl-2-docosahexaenoyl-*sn*-glycero-3-phosphatidylcholine (18:0/22:6ω3*cis* PC) bilayer-water system [52,56].

Moreover, computer simulations of three unsaturated lipids in a membrane environment: 16:0/18:1ω9*cis* PC, 1-palmitoyl-2-elaidoyl-*sn*-glycero-3-PC (16:0/18:1ω9*trans* PC) and 1-palmitoyl-2-isolinoleoyl-*sn*-glycero-3-PC (16:0/18:2ω9*cis* PC) have been carried out using Langevin dynamics (and a mean field) [57].

A Monte Carlo dynamics method [58] on a lattice was applied in a study of the effects of double bonds on the properties of lattice chains arranged in a monolayer end grafted on an impenetrable interface. The method was used in a study of model lattice bilayers of 16:0/18:1ω9*cis* PC [59] and 18:1ω9*cis*/18:1ω9*cis* PC [59,60].

Furthermore, efforts are underway to calculate the properties of isolated unsaturated chains. Monte Carlo dynamics study of hydrocarbon chains (on a lattice) consisting 18 segments and containing *cis* double bonds [61,62], of isolated 18-carbon monounsaturated chains with *cis* or *trans* double bonds [63] were reported. Brownian dynamics simulations of isolated linear chains of 18 carbons, with one, two, three (*cis* and *trans*) double bonds were performed [62]. MD studies of isolated polyunsaturated 22:6ω3*cis* chain [64], and 18:1ω9*cis*, 18:2ω6*cis*, and 20:4ω6*cis* chains [65] were carried out.

A continuum Monte Carlo (MC) model [66,67] was used in a study of various properties of many isolated unbranched lipid hydrocarbon chains with 1–6 double bonds mainly in the *cis* and also in the *trans* configuration. Both the mean end-to-end distances and the temperature coefficients of the mean-square end-to-end distances [68–70] of the unsaturated chains were calculated. The most extended (''crystal'') conformation [69,71,72] of the polyunsaturated chain has been considered. The equilibrium flexibility characteristics for hydrocarbon chains with methylene-interrupted [71–73] and non-methylene-interrupted [73,74] double bonds, the equilibrium shape [70,75,76] and some intramolecular bond-ordering characteristics [77–80] of unsaturated fatty acid chains were investigated by this MC method.

A molecular mechanics modeling approach was used to study conformational and packing properties of 22:6ω3*cis* chain [81]. The same method is used to investigate the effect of acyl chain unsaturation on both the conformation of model diacylglycerols (G) 18:0/18:1ω9*cis* G, 18:0/18:2ω6*cis* G, 18:0/18:3ω3*cis* G, 18:0/20:3ω9*cis* G, 18:0/20:4ω6*cis* G, and 18:0/22:6ω3*cis* G [82] and their packing in dense monolayers [83]. A molecular mechanics study of several structures of 16:0/18:1ω9*cis* PC [84] and 16:0/18:2ω6*cis* PC [85] molecules were performed.

A mean-field theory is yet another way to study membrane systems: the conformational properties of a single lipid molecule are the subject of the calculations in the mean-field approach, and the averaged influence of the neighboring lipid molecules on the probe molecule is considered. The statistical weight of a given conformation of a single lipid molecule is determined by weighting it by the Boltzmann factor which features the external potential field felt by this conformation. This procedure is repeated for all possible conformations of the lipid molecule and the potential fields are chosen such that they represent the other lipid molecules in the system. This approach, known as a self-consistent field (SCF) theory, makes it possible to investigate different systems and phenomena, e.g., model bilayer membranes (formed by lecithin-like molecules) [86], lipid vesicles [87], lipid bilayer membrane gel to liquid phase transition [88], inhomogeneous membrane systems [89], micellar size and shape [90], etc. Typically the SCF equations are mapped on a grid and solved numerically up to high precision. A mean-field theory was also applied to calculate the conformational properties of the unsaturated hydrocarbon chains in the hydrophobic cores of 18:1ω9*cis*/18:1ω9*cis* PC and 16:0/18:1ω9*cis* PC lipid bilayers [91]. The mean-field approach was used in the above-mentioned work [57] for the investigation

of 16:0/18:1ω9*cis* PC, 16:0/18:1ω9*trans* PC, and 16:0/18:2ω9*cis* PC molecules in a membrane environment.

It is important to mention some findings for the properties of unsaturated chains obtained by previous theoretical investigations. An increase in the number of methylene-interrupted *cis* double bonds to the maximum possible number in isolated linear hydrocarbon chain, resulted in a sharp decline of the absolute magnitudes of the chain temperature coefficient $|d \ln\langle h_0^2\rangle/dT|$ [68,69]. Here $\langle h_0^2\rangle$ is the mean-square end-to-end distance of the chain, and T is the temperature. It is expected that this property of *cis*-polyunsaturated lipid chains is exploited in biological systems. In particular, it is speculated that these lipids provide a suitable interaction with embedded enzymes. Indeed, it was found from experiment that the hexaenoic species of aminophospholipids were preferentially associated with proteins in neural membranes (see, e.g., Ref. [92]). It has been proposed that polyunsaturated aminophospholipids such as 22:6-PS or 20:4-PE may exert a regulatory role for many cellular processes; this has been confirmed, e.g., for PS and opiate receptor binding [92,93]. Such a general idea about specific lipid surroundings of embedded enzymes, which is significantly enriched with polyunsaturated acyls, has great biological significance. The theoretical predictions of low values of the temperature coefficient of the end-to-end distance for the polyunsaturated chain as compared to that for saturated chains [68] allowed us to give a more concrete, ''temperature,'' explanation of the regulatory role of polyunsaturated chains. Indeed, the hypothesis was advanced [68] that one of the possible roles of 22:6ω3*cis* and a number of other polyunsaturated chains is to thermostabilize the lipid surroundings (''lipid jacket'' [68]) of enzymes embedded in the biological membrane. This insulation can promote or maintain the active conformation of such enzymes in variable conditions. Incorporating of 22:6ω3*cis* acyls into the membrane (or redistribution of it within the membrane) may be one of the ways the cell reacts to any change in temperature [68].

Other theoretical investigations showed additional physical properties of polyunsaturated chains. It was proven that (i) polyunsaturated chains (such as 22:6ω3*cis*) are characterized by the highest equilibrium flexibility (the measure of the equilibrium flexibility was $\langle h_0\rangle/L$ [71–74], where $\langle h_0\rangle$ is mean end-to-end distance and L is the contour length of the chain), (ii) the above-mentioned size temperature sensitivity coefficient $d \ln\langle h_0^2\rangle/dT$ of the polyunsaturated molecule is ten times lower than that of a saturated chain [68–72], (iii) the polyunsaturated chain assumes with a high probability the extended, the ''angle iron-shaped,'' conformation (experimentally detected in Ref. [94]) when all the chains (saturated and polyunsaturated) are efficiently packed below the phase-transition temperatures [69,71,72,81]. As a result, a clearer formulation of the possible functions of polyunsaturated chains for embedded enzymes was offered [71,72,74]. To summarize briefly, polyunsaturated boundary lipids seem to provide the proper conditions of the proteins for their optimal functioning at different temperatures. At the same time the possible role of monounsaturated and diunsaturated chains is assumed to maintain the membrane fluidity level (for a review, see Ref. [21]). Additional characteristics of polyunsaturated chains were calculated in Refs. [64,65]. The kinetic flexibility (its measure was the frequency of conformational transitions in the torsion angles in the chains) of docosahexaene 22:6ω3*cis* [64] and arachidonic 20:4ω6*cis* fatty acid [65] was shown by MD simulations to be higher than that for the saturated chains, similar to the equilibrium flexibility [71–74].

More recently the theoretical predictions listed above were substantiated by experimental data. For example, ^{2}H nuclear magnetic resonance (NMR) works [23,25] suggested a more flexible 22:6ω3*cis* chain structure, to be contrasted to older ^{2}H NMR work [97] for 16:0/18:2ω9*cis* PC where a relatively rigid structure near the double bonds was reported. ^{2}H NMR spectroscopy was used in Ref. [23] to determine some properties for a series of PC molecules with 18:0 chain in position *sn*-1 and 18:1ω9*cis*, 18:2ω6*cis*, 18:3ω3*cis*, 20:4ω6*cis*, 20:5ω3*cis*, or 22:6ω3*cis* chain in position *sn*-2, and it was found that in highly unsaturated PCs (three or more double bonds in *sn*-2) the chain length of 18:0 was somewhat less sensitive to the temperature (see also Refs. [24,25]). From these experiments it was concluded in Ref. [7] that ''a polyunsaturated membrane may provide optimal conditions for embedded proteins over a much wider temperature range than saturated or monounsaturated membranes.'' The sense of this conclusion coincides with those formulated in our (above-mentioned) works [21,68,71,72,74]. These concepts are also found in Ref. [98] in which heterotrophic microorganisms were investigated.

Also the high chain compressibility for 22:6ω3*cis* indicated by ^{2}H NMR and x-ray diffraction study [26] is consistent with our theoretical predictions about high equilibrium and kinetic flexibilities of 22:6ω3*cis* [21,64,71–74].

Further computer simulations [77–80] and calculations of intramolecular bond-order characteristics in polyunsaturated chains allowed to establish other distinguishing features. In particular the high orientation fluctuations of C—H bonds of CH_2 group located between the *cis* double bonds have been identified (''the broadening effect'').

All the reviewed lines of investigations have contributed significantly to our understanding and further studies will undoubtedly give again more insights. The combinations of complementary methods are potentially even more exciting. Very few of such studies have been reported. In this paper, MD computer simulations, using the collision dynamics method, are applied to the investigation of hydrated bilayers of 18:0/18:1ω9*cis* PC (SOPC) and 18:0/22:6ω3*cis* PC (SDPC) in the liquid-crystal phase, and critically compared to results of a molecular-level SCF calculation for the same bilayers. One reason to consider SCF calculations is that this technique is computationally many orders of magnitude more efficient than simulations. As yet it remains unclear how good or bad this approach works for these systems. The comparative analysis will solve this issue. Both methods are known to have their limitations. The MD simulations suffer from comparatively short lengths of the simulations or/and small system sizes, huge CPU times and still inaccurate force field parameters. The SCF approach gives significantly less detailed information on the molecular system as not all

excluded-volume correlations are accounted for. Also, there is significant uncertainty about the optimal values of the interaction parameters. A combination or comparison of the methods allows us to remove, to some extent, the restrictions. One of the aims of this paper is to demonstrate the advantages of such an approach. In the following section (models and methods) one can find a detailed description of the molecular model of the lipids and bilayers, the force field and the parametrization in MD simulations. Then a short description of the SCF method is presented. The Results section contains both the data obtained on the order-parameter profiles and the comparison with the available experimental NMR data, as well as the bond orientation distribution functions, the root-mean-square (RMS) deviations of the lipid atoms from their average positions. The physical properties of unsaturated and polyunsaturated lipid tails are discussed in their biological context in the Discussion section.

II. MODELS AND METHODS

A. Molecular dynamics simulation

The main idea of MD simulations of a many-particle system is the solution of the Newton's equations of motion for a set of particles (atoms or molecules) that comprises the system. This procedure includes a model description of the atomic system, atom-atom interaction potentials, boundary conditions of the system, and an approximate step-by-step technique for solving the classical equations of motion.

The simulation cells of the two bilayers contained 96 SOPC (or SDPC) molecules and 2304 water molecules: 48 lipid molecules per layer and 24 H_2O molecules per lipid. Each lipid molecule contains a saturated (18:0) chain and an unsaturated one (Fig. 1). An initial (highly ordered) configuration of the lipids in 18:0/22:6ω3*cis* PC bilayer is shown in Fig. 2(a). The water phase consisted of explicit TIP3P water [95] molecules. The H_2O geometry [95] parameters, the partial charges [95], and the force constants [96] for H_2O are fixed. The total number of atoms in the cell was 20 352 for 18:0/18:1ω9*cis* PC bilayer and 20 544 for 18:0/22:6ω3*cis* PC bilayer. Below we will not repeat this long notation and use a short version of it, i.e., 18:0/18:1 and 18:0/22:6, respectively.

The potential energy U of a bilayer was calculated as

$$U = U_b + U_a + U_t + U_{oop} + U_{vdw} + U_e, \tag{1}$$

where U_b is the bond-stretching energy,

$$U_b = \sum K_l (l - l_0)^2, \tag{2}$$

U_a is the angle-bending energy,

$$U_a = \sum K_\Theta (\Theta - \Theta_0)^2, \tag{3}$$

U_t is the torsion energy,

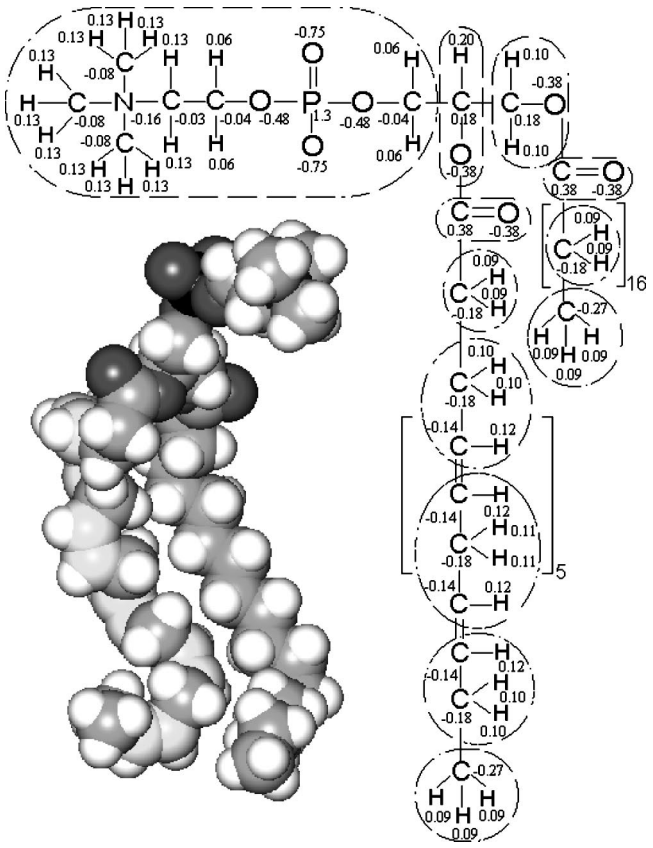

FIG. 1. Chemical structure of 1-stearoyl-2-docosahexaenoyl-*sn*-glycero-3-phosphatidylcholine (18:0/22:6ω3*cis* PC, more shortly 18:0/22:6 or SDPC). The double bonds of the unsaturated chain are located between carbon atoms 4 and 5, 7 and 8, 10–11, 13 and 14, 16 and 17, and 19 and 20. The chemical structure of 1-stearoyl-2-oleoyl-*sn*-glycero-3-phosphatidylcholine (18:0/18:1ω9*cis* PC, short hand 18:0/18:1, SOPC) has one double bond of the unsaturated chain 18:1ω9*cis* which is located between carbon atoms 9 and 10. Atom centered partial point charges in electron units for the molecular dynamics simulations are presented; the set [99] was used with consideration for the data of unsaturated lipid chains [43]. The boxes (dashed line ellipses) delineate neutral groups. A space-filling model of SDPC is also shown.

$$U_t = \sum K_\varphi [1 + \delta \cos(n_0 \varphi)], \tag{4}$$

U_{oop} is the out-of-plane energy (only for the double bonds and the carbonyl groups),

$$U_{oop} = \sum K_\phi [1 - \cos(2\phi)], \tag{5}$$

U_{vdw} is the van der Waals energy,

$$U_{vdw} = \Sigma\Sigma U_{LJ}(r_{ij}) W_{vdw}(r_{ij}),$$

where

$$U_{LJ} = 4\varepsilon_{ij}[(\sigma_{ij}/r_{ij})^{12} - (\sigma_{ij}/r_{ij})^6] \tag{6}$$

and W_{vdw} is the switching function,

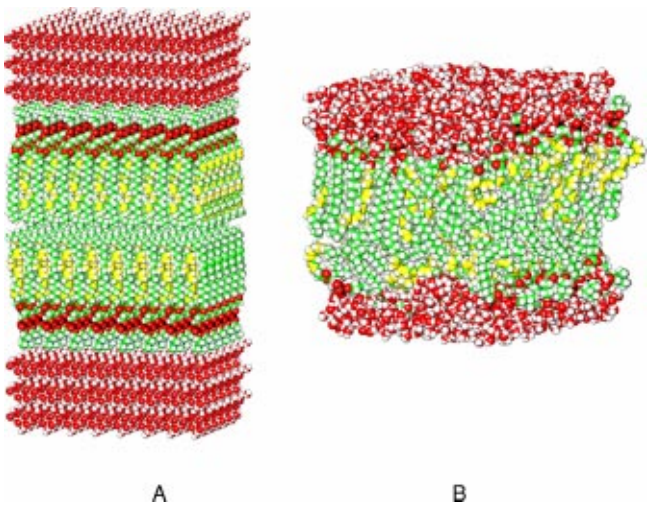

FIG. 2. (a) The initial configuration and (b) a typical snapshot for the 18:0/22:6 PC-water bilayer cell in the molecular dynamics simulations. The z axis (z is the vertical axis) is perpendicular to the two monolayers.

$$W_{vdw}(r_{ij}) = \begin{cases} 1, & r_{ij} \leqslant R_{on} \\ \dfrac{(R_{off}^2 - r_{ij}^2)^2 (R_{off}^2 - 3R_{on}^2 + 2r_{ij}^2)}{(R_{off}^2 - R_{on}^2)^3}, & R_{on} < r_{ij} < R_{off} \\ 0, & r_{ij} \geqslant R_{off}. \end{cases} \tag{7}$$

U_e is the electrostatic energy,

$$U_e = \sum \sum [q_i q_j / (\varepsilon r_{ij})] W_e(r_{ij}), \tag{8}$$

where W_e is the screening function,

$$W_e(r_{ij}) = \begin{cases} (1 - r_{ij}/R_e)^2, & r_{ij} \leqslant R_e \\ 0, & r_{ij} > R_e. \end{cases} \tag{9}$$

In Eqs. (1)–(9) the following notations are used: l is the bond length, Θ is the bond angle, φ is the torsion angle, ϕ is the out-of-plane angle, l_0, Θ_0 are equilibrium values for the bond lengths and angles; K_l, K_Θ, K_φ, K_ϕ are force constants for the bonds, angles, dihedrals, and out-of-plane angles, respectively; n_0 is the dihedral multiplicity; r_{ij} is the distance between nonbonded atoms i and j; ε_{ij}, σ_{ij} are Lennard-Jones parameters for the atom pairs, R_{on}, R_{off} are switching parameters; q_i, q_j are the partial charges on atoms i, j, ε is the dielectric constant, R_e is the screening radius.

Structural parameters for lipid molecules (bond lengths, angles, force constants) and torsion parameters were generally chosen according to the set [96] (which is close to the parameter set of Ref. [99]) and the structural data of Refs. [100,101] were also taken into account. The partial charges [99] (in electron units) were used with consideration for the data of unsaturated lipid chains [43]; the charges for 18:0/22:6 PC molecules are presented in Fig. 1, $\varepsilon = 1$, the charges for water: on the oxygen $q(OW) = -0.834$, on the proton $q(HW) = 0.417$. The parameters for nonbonded (van der Waals) interactions were borrowed from Ref. [102]. The mixing rules $\varepsilon_{ij} = (\varepsilon_{ii}\varepsilon_{jj})^{1/2}$, $\sigma_{ij} = (\sigma_{ii} + \sigma_{jj})/2$ were used, for parameters that are not explicitly given. The switching parameters $R_{on} = 0.9$ nm, $R_{off} = 0.105$ nm, $R_e = 0.105$ nm are adopted.

Equations of motion were integrated by using the "velocity Verlet" algorithm [103,104]. The simulation time step was 1 fs (10^{-15} sec). The relatively novel collisional dynamics [105] (CD) method was used. In this method the equations of motion (for N-P-T ensemble) are

$$\frac{dr_{i,\alpha}}{dt} = v_{i,\alpha} + \chi_\alpha \beta_p (P_\alpha - P_{\alpha,ref}) r_{i,\alpha}, \tag{10}$$

$$m_i \frac{dv_{i,\alpha}}{dt} = -\frac{\partial U}{\partial r_{i,\alpha}} + \sum_k f_{k,\alpha}^i \delta(t - t_k^i), \tag{11}$$

where $i = 1,2,\ldots,N$; $\alpha = \{x,y,z\}$; $\delta(t)$ is Dirac's delta; $f_{k,\alpha}^i$ and t_k^i ($k = 1,\ldots$) are impulse forces and accidental time moments of atom collisions with virtual bath particles; $r_{i,\alpha}, v_{i,\alpha}$ are the coordinates and velocities of atom i; β_p, χ_α are parameters for the pressure relaxation; $P_{\alpha,ref}$ are reference values of pressure components.

The CD thermostat is implemented by stochastic collisions with virtual particles of mass m_0: $\vec{f}_k = 2[m_0 m_i/(m_0 + m_i)](\vec{v}_0 - \vec{v}_i)$, $v_{0,\alpha}$ are chosen from a Gaussian distribution,

$$P(\vec{v}_0) = \left(\frac{m_0}{2\pi k_B T_{ref}}\right)^{3/2} \exp\left(-\frac{m_0 \vec{v}_o^{\,2}}{2k_B T_{ref}}\right), \tag{12}$$

T is instantaneous temperature of the system, T_{ref} is prescribed (bath) temperature.

The collisions occur in accordance with a Poisson process specified by a single parameter λ_0 which is the mean number of collisions that atom i suffers per unit time ("collision frequency"); $\lambda_0 = 10$, $m_0 = 1$ at. wt unit are chosen. All the details of the CD method were described previously [105].

Periodic boundary conditions in the three directions (x,y,z) were used. The bilayer systems were coupled to an external temperature bath ($T_{ref} = 303$ K) and pressure $P_{\alpha,ref}$. The simulation temperature of 303 K is higher than the relevant experimental gel to liquid-crystal phase-transition temperatures T_c [23,31,106] for these PCs ($T_c = 280$ K for 18:0/18:1 PC and $T_c = 269$ K for 18:0/22:6 PC).

The cross-sectional areas per molecule were fixed during the first 400 ps of relaxation to 0.666 nm^2 for 18:0/18:1 PC and 0.716 nm^2 for 18:0/22:6 PC, as in hydrated dispersions of pure PCs at 303 K [24]; the z pressure $P_{z,ref}$ (along the bilayer normal) was set to 1 atm at this period (400 ps). After a 400-ps relaxation trajectory (the first step) both the z pressure and the lateral pressures, $P_{\alpha,ref}$, were assigned values of 1 atm. Then another relaxation run of $\sim$200 ps was performed (the second step), in which the cross-sectional areas per molecule in the two bilayers reduced from the above-mentioned values of 0.666 and 0.716 nm^2 to respectively $\sim$0.620 and $\sim$0.695 nm^2. After the second step was com-

pleted the MD production runs of 1018 ps were executed for the calculation of all the reported characteristics. Consecutive configurations of the bilayers were sampled every 50 fs. The mean cross-sectional area during the MD simulations was equal to 0.6134 nm^2 for 18:0/18:1 PC and to 0.6624 nm^2 for 18:0/22:6 PC. Thus the simulation conditions resembled the liquid-crystalline phase of the bilayers because the simulated areas are close to those found in experiment, i.e., for lamellar liquid-crystalline bilayers of 18:0/18:1 PC and 18:0/22:6 PC in excess water cross-sectional areas per molecule 0.614 nm^2 and 0.692 nm^2 were obtained in a combined analysis of x ray and ^{2}H NMR at $T=303$ K and 0 to 8 dyn/cm lateral pressure [26].

A typical snapshot for 18:0/22:6 PC bilayer is given in Fig. 2(b). With respect to Fig. 2(a) a considerable randomization of the initially ordered structure has been realized. This is reflected in many conformational fluctuations both in the tail-, in the head-group region, as well as the water phase. Results presented below are averaged over all sampled configurations along the trajectories.

B. Self-consistent field method

The goal is to find an accurate description of thermodynamic, mechanical, and structural properties of lipid bilayer membranes. The density of lipid molecules in the bilayer membranes is very high: packing effects have a large influence on the physical properties. This means that each lipid molecule interacts with many others. This is the ideal situation for a mean-field theory to be reasonably accurate. The performance of the mean-field approach then relies on the accuracy by which the size and shape (chain architecture) of the lipid molecules is represented. At the same time it is necessary to account for the short- and long-range interactions. For example, the two hydrophobic tails should prefer their own (apolar) environment over that of the water phase. The zwitter-ionic head group is expected to prefer the medium with high dielectric permittivity.

Here we use a molecular level SCF approach applying the discretization scheme of Scheutjens and Fleer [86–90,107,108]. All essential details of the SCF calculations are presented in a paper [109] where also an extensive discussion on the choices for the various parameters can be found. At this point it suffices to mention that the molecules are represented on a united atom level. The units (segments) interact by nearest-neighbor contacts using Flory-Huggins parameters. Electrostatic interactions are included on the level of the Poisson-Boltzmann equation [110,111]. Chain conformations are described in a rotational isomeric state model. The *cis* double bonds are modeled by forcing a local gauche conformation in the chain. Water molecules are assumed to form (local) clusters with variable size [109]. The association constant K mimics the action of H bonds. Finally, it is necessary to allow for free volume in the system [109]. At ambient pressure, the free volume is allowed to distribute according to the interaction parameters used in the system.

The accurate self-consistent-field solution is generated numerically. Typically we obtain at least seven significant digits for the densities in the system. The next step is to obtain the grand potential, or equivalently the surface tension of the bilayer. If the surface tension is finite, we restart the computations with a new value of the number of lipids per unit area. Typically this procedure is repeated until the absolute value of the surface tension is less than 10^{-5} (in dimensionless units). Only results of tension-free bilayers are presented below. Mechanical parameter of the bilayers, such as the membrane compressibility, the Helfrich parameters, etc., can be computed [112,113], but in this paper the structural properties will be highlighted. Unlike primitive mean-field calculations for surfactant systems, where the tails are grafted to some plane, we have no restrictions on the molecules. Each molecule is free to partition between the bulk and the membrane. Indeed the concentration of free lipid molecules in the bulk is close to the critical micellization concentration for the lipids under investigation.

III. RESULTS

In this paper the main focus points are the C—H bond-order parameters, the bond orientation probability distribution functions, and the root-mean-square values of the fluctuations of the acyl carbons. These quantities are sensitive to the degree of unsaturation in the chains.

A. C—H bond-order parameters

The C—H bond-order-parameter $-S_{CH}$ profiles, given by

$$S_{CH}=(3<\cos^2\beta_{CH}>-1)/2, \tag{13}$$

are presented in Fig. 3. Here β_{CH} is the angle between the bond C—H and the bilayer normal. When the bond-order parameter $S=1$, the bond is parallel to the bilayer normal and when $S=-0.5$, the bond is perpendicular to it. The inverse is also true, i.e., if the bond is parallel to the bilayer normal, the order parameter $S=1$, and if the bond is perpendicular to the bilayer normal, the order parameter $S=-0.5$. Furthermore, if the bond does not show any preferred orientation, the order parameter is zero, $S=0$. However, an S that equals 0 does not necessarily mean that the bond orientation distribution is full isotropic: a value of order parameter $S=0$ can result from different bond orientation distributions.

In Fig. 4 the order-parameter profiles obtained by SCF calculations are given for both tails of lipid molecules of these bilayers. The order parameter is easily computed in the SCF model from the information on the direction of the bonds connected to the segment along the chain (for more details of the SCF model, see Ref. [110]). In this model, the $S_{CH}(t)$ order parameter is unity when the bond between segments $t-1$ and t is in the normal direction. When for all molecules in the system this bond is in the plane of the bilayer, the order parameter is -0.5. For a random distribution, of course, a value of zero is found.

The $-S_{CH}$ order-parameter profiles for both the saturated and monounsaturated chains of 18:0/18:1 PC bilayer (Figs. 3 and 4) are in reasonable agreement with experimental values [114]. The $-S_{CH}$ order-parameter values of the double-bonded carbons of unsaturated chain of 18:1 significantly differ from one another, the shape of the calculated profile of

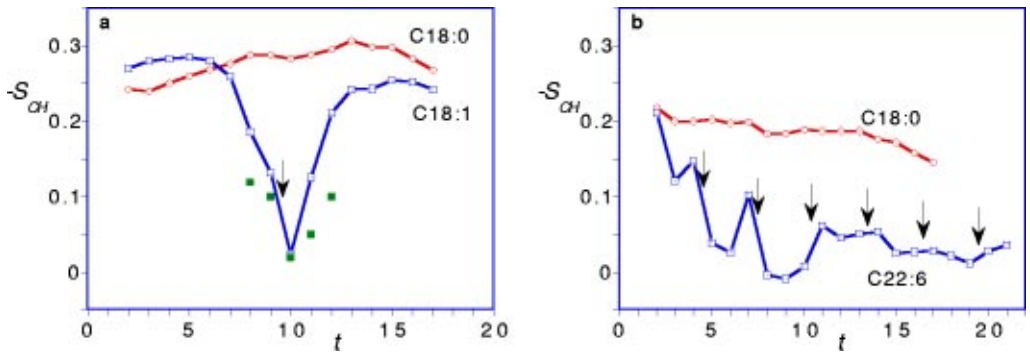

FIG. 3. The $-S_{\mathrm{CH}}$ order parameter as a function of the carbon number t of the lipid hydrocarbon chains of the bilayers (a) 18:0/18:1 PC and (b) 18:0/22:6 PC at 303 K as determined from the MD simulations (see text). In plot (a) some experimental data for the deuterium order parameter, $|S_{\mathrm{CD}}|$, with the segment position in the region of the double bonds for the oleoyl chain (18:1)exp of bilayers of 16:0/18:1 PC is given [114] (at 300 K). The arrows indicate the double-bond positions. The calculated $-S_{\mathrm{CH}}$ values are averaged over the two C—H bonds of CH_2 groups. To calculate the profiles, the trajectory of 1018 ps was computed for 18:0/18:1 PC bilayer (the average area per molecule was 0.6134 nm^2) and 1018 ps for 18:0/22:6 PC bilayer (0.6624 nm^2).

the *cis* double-bond region is quite similar to the experimental one. The dip in the order-parameter profile of 18:1 chain near the region of double-bonded carbons was also observed in other computer simulations with monounsaturated acyls [38–43,45–47,58–60] and mean-field calculations [57,91]. Besides, it is significant to point to the fact that in the SCF calculations of SOPC bilayer the order in the *sn*-2 monounsaturated chain is a bit higher than in the *sn*-1 saturated chain for the tail segments $t=2$–5 (Fig. 4). This may be attributed to the fact that the *sn*-2 chain has to ''catch-up'' with the *sn*-1 chain, because it starts at a slightly higher z coordinate. The same effect for carbons 2–5 of *sn*-2 chain of the bilayer 18:0/18:1 PC is found in the MD calculations; however, all the $-S_{\mathrm{CH}}$ values in the *sn*-2 chain of the bilayer 18:0/22:6 PC are lower than those for *sn*-1 chain (Fig. 3). Thus, even with a single *cis* double bond in the lipid chain the bond-ordering picture in the unsaturated bilayer differs significantly from that of the saturated one. The order-parameter profile of the saturated chain (18:0) exhibits a ''plateau,'' the order drops gradually to the chain end (depending on specific conditions). The average magnitude $(|S_{\mathrm{CH}}|)_{av}$ of the C—H bond-order parameter of the hydrocarbon lipid chain of the bilayer given by

$$(|S_{\mathrm{CH}}|)_{av}=[1/(N-2)]\sum_{k=2}^{N-1}|S_{\mathrm{CH}}|, \tag{14}$$

where N is the total number of the chain carbons ($N=18$ or 22 for our lipid chains), decreases when the chain unsaturation in the bilayer increases from one to six double bonds. In the MD calculations for the PC bilayers, $(|S_{\mathrm{CH}}|)_{av}$ is equal to 0.223 for 18:1 chain and 0.053 for 22:6 chain. The corresponding values found by the SCF calculations are 0.251 (18:1) and 0.099 (22:6), which are systematically slightly higher. These results correspond nicely to our MD simulations with DG monolayers [47] in which the values $(|S_{\mathrm{CH}}|)_{av}$ were 0.106 and 0.025 for the unsaturated chains in the monolayers of 18:0/18:1ω9*cis* DG and 18:0/22:6ω3*cis* DG, respectively [47] (see also the bond-order-parameter profiles in Refs. [45,46]).

The average order parameter of the 18:0 chains is higher for the 18:0/18:1 lipid bilayer than for the the 18:0/22:6 bilayer as is clear from both the MD (Fig. 3) and SCF (Fig. 4) results. This drop in the average order of the saturated chain correlates with the area per molecule in both cases. Above it was shown that the area per molecule increases with increasing degree of unsaturation in the acyl chains. A large area per

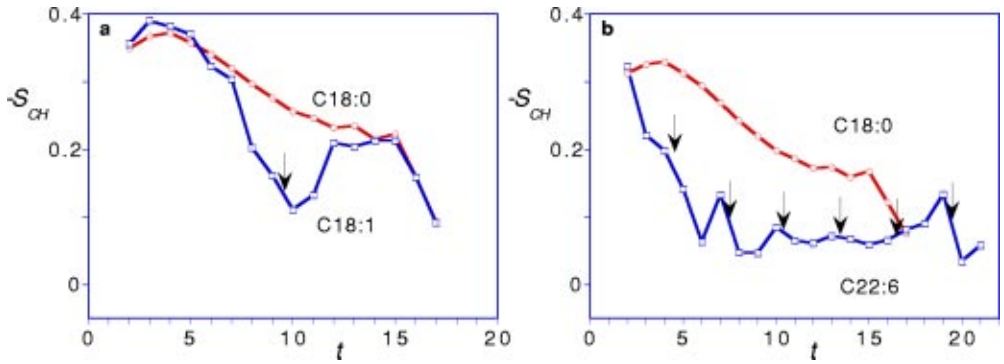

FIG. 4. Order-parameter profiles $-S_{\mathrm{CH}}$ for both tails of the lipid molecules of SOPC and SDPC as determined from the SCF calculations; t is the segment number along the chain. The arrows indicate the positions of double bonds.

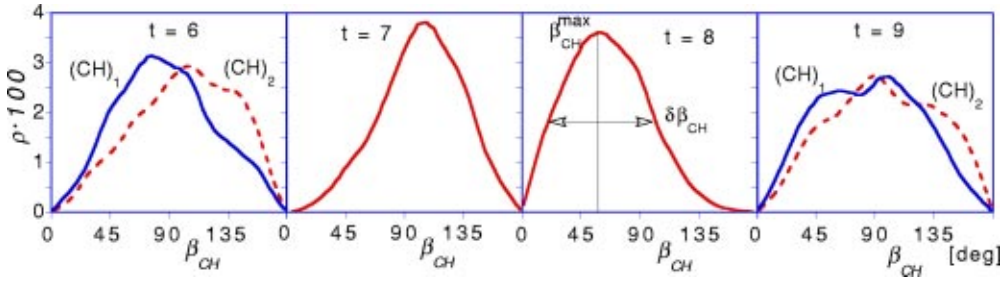

FIG. 5. Histograms of several C—H bond-vector orientation distributions $\rho_{CH}(\beta_{CH})$ of the chain 22:6 relative to the bilayer 18:0/22:6 PC normal; $t=6,7,8,$ and 9 are carbon numbers of the 22:6 chain. Each of the distributions contains 60 calculation points (MD simulations). For the eighth carbon, the angle β_{CH}^{max} value (β_{CH}^{max} corresponds to the maximum of the distribution) and the distribution width $\delta\beta_{CH}$ (full width at half maximum) are indicated.

molecule allows for more freedom for the chains to adopt various conformations other than the fully stretched one. It must be understood, that in both models (SCF and MD) the area per molecule is not an input parameter but a prediction of the calculations and thus this correlation is significant.

The profile of $-S_{CH}$ obtained in this work for the lipid bilayer chain with six double bonds should be considered as a theoretical prediction (see also Refs. [47,48,52,56]) because, to our knowledge, experimental data on the order-parameter profile of the polyunsaturated 22:6 chain in bilayer membranes is not available.

B. C—H bond orientation distribution functions

From the bond-order-parameter profiles (such as in Figs. 3 and 4), it is impossible to determine the exact (unique) ordering picture of a particular bond, especially because the order parameter S of a given bond is not equal to 1 or -0.5. In the general case a bond orientation probability distribution function $\rho_{CH}(\beta_{CH},\psi_{CH})$, where the angles β_{CH} and ψ_{CH} are the polar coordinates of the C—H bond vector with respect to the bilayer normal (ψ_{CH} is the angle in the bilayer surface), gives a much more detailed description of the C-H vector ordering. Let $\beta_{CH}=\beta$, $\psi_{CH}=\psi$, then the bond distribution function is defined as

$$\rho_{CH}(\beta_{CH},\psi_{CH})=\frac{\exp[-U(\beta,\psi)/k_BT]}{\int_0^{\pi}\int_0^{2\pi}\exp[-U(\beta,\psi)/k_BT]\sin\beta d\beta d\psi}, \tag{15}$$

where k_B is Boltzmann constant, T is the temperature. Integration over the angle $\psi_{CH}=\psi$ in the bilayer surface leads to the orientational distribution $\rho_{CH}(\beta_{CH})$ given by

$$\rho_{CH}(\beta_{CH})=\frac{\sin\beta\int_0^{2\pi}\exp[-U(\beta,\psi)/k_BT]d\psi}{\int_0^{\pi}\int_0^{2\pi}\exp[-U(\beta,\psi)/k_BT]\sin\beta d\beta d\psi}. \tag{16}$$

In this work, the distributions $\rho_{CH}(\beta_{CH})$ of all the C—H bonds of saturated and unsaturated lipid hydrocarbon chains of the two bilayers were calculated numerically by the MD simulations. Since the S_{CH} order parameter depends solely on the angle β_{CH} between the bond and the bilayer normal, only the β_{CH} dependence of the ρ_{CH} distributions was investigated in this work, similar to those investigated previously for DG monolayers [45–47] and for isolated hydrocarbon chain molecules with respect to the molecule principal axis of inertia [77–80]. For the computation of the distribution functions, the angle β_{CH} in the range 0°–180° of each C—H bond was divided into 60 sectors (j) of 3° each: 0°–3°, 3°–6°, . . . , 177°–180°, as was done in Refs. [45–47,77–80].

Both 0° and 180° mean parallel to the membrane normal and 90° means parallel to the membrane surface. Then the percentage that the angle β_{CH} appears to be in the jth sector ($j=1,2,\ldots\ldots,60$) was recorded. The final functions $\rho_{CH}(\beta_{CH})$ of each CH_2 group were found by averaging over the two C—H bonds in the group. The distribution $\rho_{CH}(\beta_{CH})$ of the given bond was averaged over all the molecules in the two monolayers of the bilayer.

For completeness we present in Fig. 5 several distributions $\rho_{CH}(\beta_{CH})$ calculated for an acyl tail with six double bonds, i.e., the 22:6 chain; the distributions for each C—H bond of CH_2 groups are shown separately. It is necessary to reduce the data for the subsequent discussion. To this end, all the $\rho_{CH}(\beta_{CH})$ distributions to the S_{CH} parameters for the two bilayers were analyzed in terms of the angle for which $\rho_{CH}(\beta_{CH})$ has its maximum β_{CH}^{max} and the width $\delta\beta_{CH}$ corresponding to the difference in angle for the half heights of the distributions $\rho_{CH}(\beta_{CH})$, i.e., full width at half maximum, as was done in Refs. [45–47,77–80]. Some of the distributions turned out to be ''bimodal'' (such as $t=6,9$ in Fig. 5). The peaks of the bimodal distributions are not fully separated: in most cases the distribution curves are not ''double-humped waves'' but contain a main peak and a small plateau region. All the angles β_{CH}^{max} and widths $\delta\beta_{CH}$ of the distributions of the PC bilayers were calculated without considering the phenomenon of bimodality: the angles β_{CH}^{max} refer to the main peaks. The results of this reduction of the data are shown in Fig. 6.

The values of β_{CH}^{max} and $\delta\beta_{CH}$ may be used to judge the ''geometric'' and ''fluctuation'' contributions to the $-S_{CH}$ order parameter. Indeed, the $\delta\beta_{CH}$ values of the C—H bonds of the double-bonded carbon atoms in the chain 18:1 are

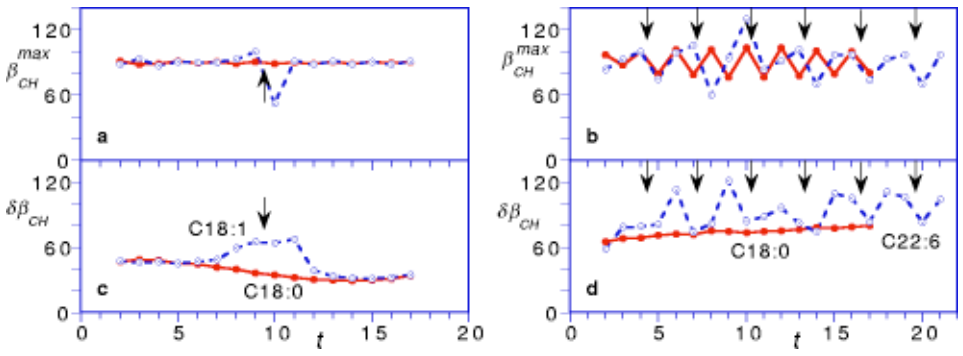

FIG. 6. MD computer simulations results for the calculated angle values β_{CH}^{max} which correspond to the C—H bond-vector distribution function maxima $[\rho_{CH}(\beta_{CH})]_{max}$ of the lipid hydrocarbon chains of the 18:0/18:1 PC (a) and 18:0/22:6 PC (b) bilayers; The calculated values of C—H bond-vector distribution function widths $\delta\beta_{CH}$ which correspond to half heights $[\rho_{CH}(\beta_{CH}^{max})]/2$ of the distributions $\rho_{CH}(\beta_{CH})$, for the hydrocarbon chains of the lipid bilayers of 18:0/18:1 PC (c) and 18:0/22:6 PC (d). The arrows indicate the double-bond positions. Accuracy is within the symbol size.

approximately equal [65.7° and 64.6° for carbons 9 and 10, Figs. 6(a),(b)] but $\beta_{CH}^{max}=100.5°$ for carbon 9 and 52.5° for carbon 10 of 18:1-chain, Figs. 6(c),(d). Hence the values of the difference $|90°-\beta_{CH}^{max}|$ are equal to 10.5° and 37.5° for carbons 9, 10, respectively. So the dip in the $-S_{CH}$ order-parameter profile of the chain 18:1 in Fig. 3 is in this case due to a pure geometric effect. The same situation is observed, e.g., for carbons 4 and 5 in the 22:6 chain. On the other hand, an opposite example can also be given: in the 22:6 chain the magnitude of the difference $|90°-\beta_{CH}^{max}|$ $=3.0°$ and 4.5° for carbons 3 and 9, however, $\delta\beta_{CH}$ $=78.9°$ and 121.1°, respectively. Figure 3 shows that the disparity in the $-S_{CH}$ values of carbons 3 and 9 in the 22:6 chain is significant. This is then due to a pure fluctuation effect. Of course many ''intermediate'' cases are observed. From this it is clear that the order-parameter profile by itself cannot give such an information.

The most important result obtained in the investigation of bond orientation probability distribution functions $\rho_{CH}(\beta_{CH})$ seems to be the ''broadening effect'': the width $\delta\beta_{CH}$ of the distribution function of the CH_2 groups located between the *cis* double bonds in polyunsaturated 22:6 chain (Fig. 6, carbons 6, 9, 12, 15, 18) is higher than that for C—H bonds of double-bonded carbons. This effect was first detected for isolated polyunsaturated hydrocarbon chains by Monte Carlo simulations [77–80] and then for monolayers consisted of polyunsaturated molecules of DGs by MD simulations [45–47].

Let us consider the C—C bond order profiles for the two bilayers. Figure 7 shows marked differences in the S_{CC} order parameter between odd and even running numbers for hydrocarbon chains of the bilayers. The odd-even effect for saturated chains is well known: this is because the rotations of the CH_2 groups about their local axes are anisotropic. The difference in behavior and properties of unsaturated lipids is that the S_{CC} order parameters of the *cis* double bond C═C in 18:1 and 22:6 chains are higher than those of adjacent single C—C bonds (see also the profiles in Refs. [49–51]).

C. RMS deviations of the acyl chain carbon positions

The root-mean-square values of the fluctuations of the acyl carbons of the 18:0/18:1 PC and 18:0/22:6 PC bilayers in ''plane'' (xy), out of plane (in the z direction) and the sum were obtained by the MD simulations and shown in Fig. 8. These fluctuations were calculated and averaged for each chain carbon atom of each molecule in the bilayer. Figure 8 shows that the RMS fluctuations of the saturated and unsaturated hydrocarbon chains of each bilayer have many similar characteristics with the exception of the region of double

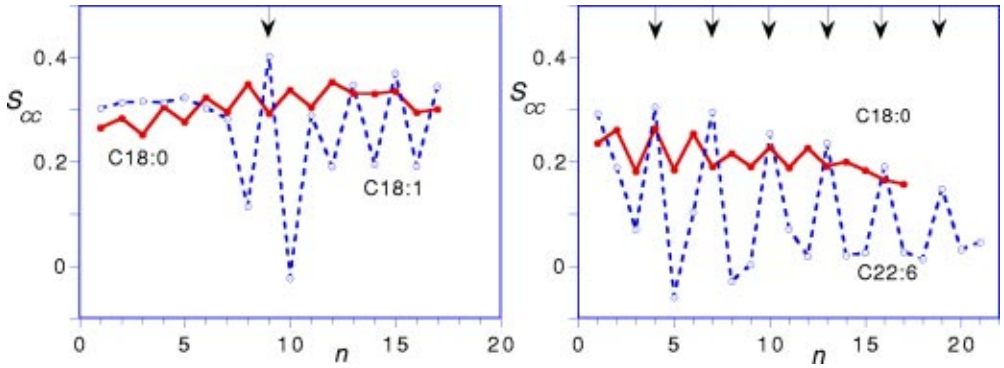

FIG. 7. Order parameter S_{CC} as a function of the bond number n of the lipid hydrocarbon chains of the bilayers as determined from the MD simulations. The arrows indicate the double bonds.

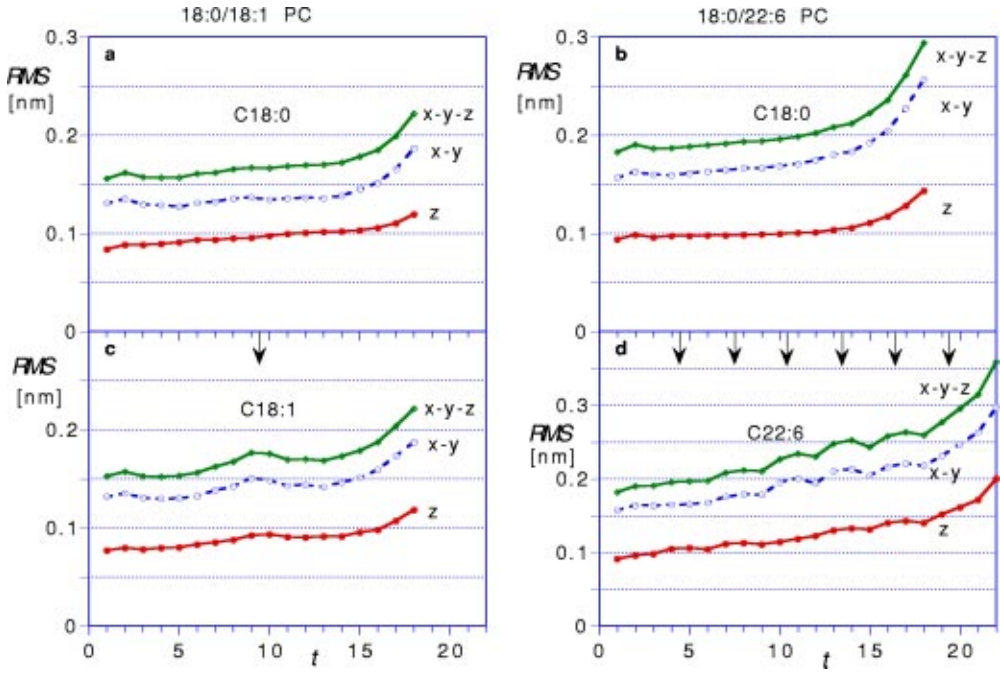

FIG. 8. Profiles of the root-mean-square values (RMS) of the positional fluctuations of the carbons of lipid hydrocarbon chains of the bilayers 18:0/18:1 PC and 18:0/22:6 PC as determined from the MD computer simulations (see text). The in-plane RMS_{xy}, the out-of-plane RMS_z, and the overall fluctuations RMS_{xyz}. The arrows indicate the double-bond positions. The RMS values were obtained using the trajectory of 1018 ps for 18:0/18:1 PC bilayer (the area per molecule was 0.6134 nm^2) and 1018 ps for 18:0/22:6 PC bilayer (0.6624 nm^2); $T=303$ K.

bonds. The difference in the profile of RMS values of this region is significant, the fluctuations of the unsaturated chain carbons are always higher than those of saturated one. The difference in the RMS fluctuations of the saturated 18:0 and polyunsaturated 22:6 lipid tails in the bilayer 18:0/22:6 PC is more than that for 18:0 and 18:1 chains in the bilayer 18:0/18:1 PC. The RMS fluctuations of the carbons of the double bonds proved to be increased as compared to the adjacent single-bonded carbons of the same chain. Also, the RMS value increases from the lipid head towards the ends of the tails. This means that the conformational entropy of tail ends is higher than that of chain fragments near the glycerol backbone.

The fluctuations in the z direction, RMS_z, of all carbons in the chains are presented as a function of the average z positions in Fig. 9. The MD simulations show that the average z positions of the end carbons of polyunsaturated sn-2 chains of the first and the second monolayers of the bilayer 18:0/22:6 PC are well separated whereas those of sn-1 chains are situated not far from each other in the center of the bilayer. In other words, it is the saturated sn-1 chain that binds the two monolayers to each other. This tail interdigitates by way of conformational fluctuations into the opposite monolayer. The polyunsaturated tail penetrates less into the opposite layer. Thus, the sn-1 and sn-2 tails do not have the same function, e.g., with respect to the bilayer thickness control. This effect has less significance in the bilayer 18:0/18:1 PC.

Figure 10 shows the average z position of segment and the RMS deviations from the average z position calculated by

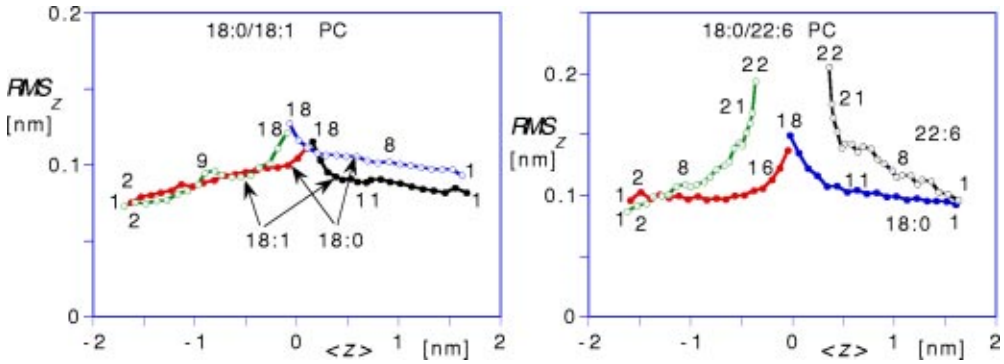

FIG. 9. The root-mean-square values RMS_z of the positional fluctuations of the carbons of lipid hydrocarbon chains of the bilayers 18:0/18:1 PC and 18:0/22:6 PC as a function of their average z positions (along the normal) as determined from the MD computer simulations (see text). Various numbers of the tail carbons are indicated.

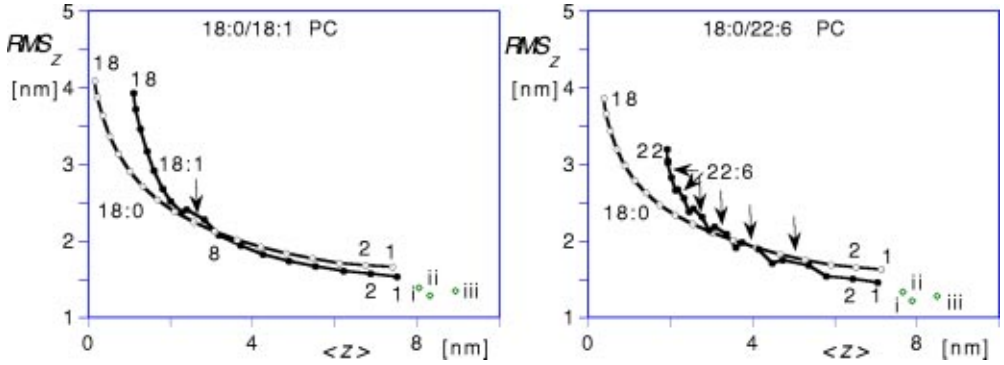

FIG. 10. SCF predictions for the *z*-component root-mean-square deviation of each segment of the two acyl chains and for the glycerol backbone units of the bilayers 18:0/18:1 PC and 18:0/22:6 PC plotted as a function of the average $\langle z \rangle$ position of these segments. Both the RMS values and the average *z* position are in units of the lattice sites (≈ 0.2–0.3 nm). The *sn*-1 tail is given by the open sphere, the *sn*-2 tail is given by the closed symbols. The glycerol backbone units are indicated by the open diamonds. Various numbers of the tail segments are indicated and the arrows point to the positions of the double bonds.

the SCF method for both the 18:0/18:1 PC and 18:0/22:6 PC bilayers. In this figure only one side of the bilayer is drawn and the bilayer center is exactly at $z=0$; unlike in simulations, the second monolayer is exactly identical to the one shown. The segments with a low ranking number are near the glycerol backbone, they have relatively high-average *z* positions (they are positioned on the outside of the bilayer) and the fluctuations are low. For segments with a high ranking number the opposite is true, they are on average positioned near the center of the bilayer and the fluctuations are high, much as for RMS_z of MD results presented in Fig. 9. For low ranking numbers the SCF method indicates that the saturated *sn*-1 chain has slightly more fluctuations and is systematically positioned slightly deeper into the bilayer (Fig. 10). This correlates with the average positions and fluctuations of the corresponding glycerol backbone units. In passing we note that for the middle glycerol backbone unit (ii) the fluctuations are the lowest in the whole molecule. Furthermore, the fluctuations typically increase near the *cis* double bond in the unsaturated *sn*-2 chain, in accordance with the result of the MD simulations (Fig. 9) but does not increase as much for the segment just after the double bond. We find that this result is natural because one of the possible roles of lipid chain unsaturation is to disturb the order inside the bilayer such that the membrane remains fluid. For the remainder of the chain the fluctuations of *sn*-2 chain are significantly higher than segments of the *sn*-1 chain positioned at the same mean position. In line with the MD results, the *sn*-2 chain does not penetrate as deep into the bilayer as the saturated *sn*-1 chain. Indeed this is a dramatic effect with many potential implications. For example, the average position of C_{11} of the *sn*-2 chain almost equals that of C_{10} of *sn*-1 (of the 18:0/18:1 bilayer in Fig. 10). The unsaturated chain is more ordered for $t<9$ than for $t>11$. Thus the double bond located in the position $t=9$ exerts some disordering influence not only locally, on the region of C_9—C_{10} of the chain, but on the remaining part of the chain (for $t>11$) as well. The same effects are seen for the chain with multiple double bonds. Indeed, although the 22:6 chain is much longer than the 18:0 chain, the chain end of the 22:6 chain does not reach as far into the bilayer as the 18:0 chain.

Comparison between Figs. 9 and 10 shows that the SCF calculations systematically show relatively large RMS values for the *sn*-1 chain. The RMS values increase more gradually towards the chain ends in the SCF results than found in the MD simulations. As a result, the highest fluctuations found in the SCF calculations is for the chain end of the 18:0 chain, whereas in the MD simulations the unsaturated chain is fluctuating most.

The RMS deviations of positions of the lipid atoms for monounsaturated 16:0/18:1 PC bilayer were calculated previously by MD simulation in the work [38], and the RMS values are relatively high for double-bonded carbons compared to the saturated chain. This increase was called the ''C═C effect'' [38]. Mention should also be made of mean-field calculations in the work [91]. The opposite result is represented in this work, i.e., the RMS deviation decreased for the double-bonded carbons of the same monounsaturated 16:0/18:1 PC bilayer [91]. It is difficult to discover the cause of this discrepancy at this moment. The RMS fluctuations of saturated 16:0 and diunsaturated 18:2 chain carbons of the 16:0/18:2 PC bilayer as a function of their mean position along the bilayer normal calculated by another MD simulation [54] revealed that the 18:2 chain segments had larger fluctuations at the same height (*z*) than those of 16:0 chain. At the same time, the fluctuations of the unsaturated 18:2 chain segments as a function of the segment number proved to be less than of the saturated (16:0) one [54].

In summary, our MD calculations (Figs. 8 and 9) revealed the RMS deviation increase (both RMS in plane and RMS out of plane and RMS total) of the carbons of double-bond regions for the two bilayers investigated, 18:0/18:1 PC and 18:0/22:6 PC, and the same is observed for the SCF modeling results (Fig. 10) and for the DG lipid bilayers, see Ref. [52].

IV. DISCUSSION

The MD simulation and the SCF modeling results provide a wealth of detailed information on the structural properties of the unsaturated bilayers. The obtained data point to the

physical properties that are characteristic for polyunsaturated lipid acyls. Some of the results confirm previously obtained data and other results add to our knowledge.

All-atom MD simulation and the SCF modeling of the hydrated unsaturated and polyunsaturated PC lipid bilayers in the liquid-crystalline phase indicate that the *cis* double bond strongly affects the local order in the bilayer. In accordance to experimental findings, the $-S_{CH}$ order-parameter profile shows a pronounced dip near the double bond. Multiple methylene-interrupted double bonds of the chain reduce the $-S_{CH}$ order-parameter values along most of the chain. The order parameters for S_{CC} of single C—C bonds next to the *cis* double bond in the unsaturated chain are lower than those for the double bonds C═C, and for the single bonds C—C at the same position along the saturated acyl chains.

A C═C effect for the root-mean-square values of the positional fluctuations of the carbons, and a broadening effect for angular fluctuations of C—H bonds of CH_2 groups in the unsaturated PC bilayers are detected. It is evident that high orientation fluctuations of C—H bonds (which are characterized by the orientation distribution function width $\delta\beta_{CH}$) of CH_2 group located between the *cis* double bonds in polyunsaturated chains with respect to the bilayer normal (i.e., the broadening effect) should be connected with high spatial fluctuations of the adjacent double-bonded carbons (i.e., with the C═C effect; the latter for the PC bilayers is similar to that of the DG bilayers [52]). The broadening effect and the order parameters for the PC bilayers are in agreement with the results of our MD calculations of the C—H bond orientation distribution functions and order parameters with respect to the normal of unsaturated DG monolayers [45–47] and DG bilayers [52].

The bond-order parameters and orientation distribution characteristics of the chains in the lipid monolayer and bilayer ''liquid'' regions, as found in experiments and in MD computer simulation models [45–47,52], are qualitatively similar to the intramolecular order parameters and the intramolecular bond orientation distributions in single unperturbed [100] unsaturated hydrocarbon chains previously investigated by the Monte Carlo simulations [77–80]. This indicates that the behavior of the acyl chains in the liquid region of lipid bilayers (somewhat remote from the membrane-water interface) is dominated by the intramolecular short-range interactions because unperturbed hydrocarbon chain properties are fully defined by the short-range interaction energy [100]. The long-range interactions of the segments of the lipids in this region of the bilayer and the interactions with the bilayer-water interface may be considered as a disturbance: the intermolecular interactions are largely used to orient the lipid molecules in the direction of the membrane normal.

All the investigations carried out by the MD and SCF approach prove that the ordering picture in the unsaturated lipid bilayers is quite complex. Many different details are observed depending on specific conditions—area per molecule, pressure, temperature etc. At the same time the main qualitatively characteristic features of the profiles of $-S_{CH}$, S_{CC}, β_{CH}^{max}, $\delta\beta_{CH}$, RMS deviations of atoms for a given acyl chain of the bilayer are together highly characteristic for the level of unsaturation, they are like fingerprints pointing one to one to the details of the unsaturation along the chain. In other words, a close relationship between the investigated characteristics (order parameters, fluctuations, etc.) and the structure of the chains is elucidated. The number of the chain carbons, the number of *cis* double bonds and their position in the chain determine principally the properties calculated: they are similar both for the bilayers of PC, DG, and the DG monolayers.

After the submission of this manuscript a combined NMR and MD simulation work [115] on $16{:}0/22{:}6\omega3cis$ PC bilayer, and a combined quantum mechanical, empirical force field calculation and MD simulation work [116] on $18{:}0/22{:}6\omega3cis$ PC bilayer were published. The order-parameter profiles obtained for $22{:}6\omega3cis$ chains are in line with the MD simulations of the present work and those of Refs. [47,48,52,56]. The findings discussed in the present work occur also in the unsaturated lipid bilayers with 2, 3, and 4 *cis* double bonds in the chains [117].

The understanding of the molecular basis of the physical properties of the lipids allows one to narrow down the list of hypotheses under consideration about the possible function of various acyls in lipid membranes. The data obtained in this work substantiated the broadening effect and elucidated high spatial fluctuations of the adjacent double-bonded carbons. So the flexibility of polyunsaturated chains is not only high on the whole [71–74] but is also evenly distributed along the chain. This is a considerable evidence in favor of our concepts [21,68,71,72,74] because the flexibility of the chain molecule which is high along the chain gives a gain in the energy of the lipid-protein interactions at the contact (boundary) surface of the lipid and protein molecules.

The MD results have given guidelines to design a significantly better parameter set for the SCF calculations. For this improved parametrization the SCF results show qualitatively the same effects of unsaturation on the local order in the bilayers. The MD results show that the computationally efficient and approximate SCF theory gives a less detailed, but nevertheless consistent, picture of the bilayers. The SCF theory can successfully reproduce single-chain properties because of the above-mentioned importance of the intramolecular short-range interactions. Even the subtle effects of chain unsaturation are recognized. This observation is relevant because the SCF analysis may be used to help understand the influence of molecular structure in relation to the bilayer properties, as this method may give direct access to thermodynamic and mechanical [112,113] properties of these layers. This in turn may be important to understand (predict) membrane properties on much longer length scales, i.e., 10–100 nm.

ACKNOWLEDGMENTS

This work was partially supported by NWO Dutch-Russian program for polyelectrolytes in complex fluids and Russian Foundation for Basic Research Grant Nos. 00-03-33181 and 01-04-48050.

[1] A.L. Lehninger, D.L. Nelson, and M. M. Cox, *Principles of Biochemistry* (Worth, New York, 1993).
[2] S.G. Wilkinson, in *Microbial Lipids*, edited by C. Ratledge and S.G. Wilkinson (Academic Press, London, 1988), Vol. 1, pp. 299–457.
[3] D.J. Murphy, Biochim. Biophys. Acta **864**, 33 (1986).
[4] G. Laskay and E. Lehoczki, Biochim. Biophys. Acta, **849**, 77 (1986).
[5] R.E. Anderson, P.J. O'Brien, R.D. Wiegand, C.A. Koutz, and A. M. Stinson, in *Neurobiology of Essential Fatty Acids*, edited by N.G. Bazan *et al.*, (Plenum Press, New York, 1992), pp. 285-294.
[6] N.G. Bazan, W.C. Gordon, and E.B. Rodriguez de Turco, in *Neurobiology of Essential Fatty Acids*, edited by N.G. Bazan *et al.* (Plenum Press, New York, 1992), pp. 295–306.
[7] D.C. Mitchell, K. Gawrisch, B.J. Litman, and N. Salem, Jr., Biochem. Soc. Trans. **26**, 365 (1998).
[8] N.G. Bazan, in *Nutrition and the Brain*, edited by R.J. Wurtman and J.J. Wurtman (Raven, New York, 1990), Vol. 8, pp. 1–24.
[9] J.M. Naughton, Int. J. Biochem. **13**, 21 (1981).
[10] G.J. Anderson and W.E. Connor, Lipids **23**, 286 (1988).
[11] A.R. Neill and C.J. Musters, Biochim. Biophys. Acta **127**, 375 (1972).
[12] R.M. Shulman and G.E. Love, *The Biochemical Ecology of Marine Fishes. Advances in Marine Biology* (Academic Press, San Diego, 1999), Vol. 36.
[13] J. Tinoco, Prog. Lipid Res. **21**, 1 (1982).
[14] C.D. Stubbs and A.D. Smith, Biochim. Biophys. Acta **779**, 89 (1984).
[15] R.R. Brenner, Prog. Lipid Res. **23**, 69 (1984).
[16] N. Salem Jr., H.-Y. Kim, and J.A. Yergey, in *The Health Effects of Polyunsaturated Fatty Acids in Seafoods*, edited by A.P. Simopoulous, R.R. Kifer, and R.E. Martin (Academic Press, New York, 1986), pp. 263–317.
[17] E.A. Dratz and A.J. Deese, in *The Health Effects of Polyunsaturated Fatty Acids in Seafoods*, edited by A.P. Simopoulous, R.R. Kifer, and R.E. Martin (Academic Press, New York, 1986), pp. 319–351.
[18] M.V. Bell, R.J. Henderson, and J.R. Sargent, Comp. Biochem. Physiol. B **83**, 711 (1986).
[19] M. Neuringer, G.J. Anderson, and W.E. Connor, Annu. Rev. Nutr. **8**, 517 (1988).
[20] P.J. Quinn, F. Joo, and L. Vigh, Prog. Biophys. Mol. Biol. **53**, 71 (1989).
[21] A.L. Rabinovich and P.O. Ripatti, Usp. Sovrem. Biol. **114**, 581 (1994).
[22] S. Everts and J.H. Davis, Biophys. J. **79**, 885 (2000).
[23] L.L. Holte, S.A. Peter, T.M. Sinnwell, and K. Gawrisch, Biophys. J. **68**, 2396 (1995).
[24] F. Separovic and K. Gawrisch, Biophys. J. **71**, 274 (1996).
[25] L.L. Holte, F. Separovic, and K. Gawrisch, Lipids **31**, s199 (1996).
[26] B.W. Koenig, H.H. Strey, and K. Gawrisch, Biophys. J. **73**, 1954 (1997).
[27] M.C. Wiener and S.H. White, Biophys. J. **61**, 434 (1992).
[28] S.J. Slater, M.B. Kelly, M.D. Yeager, J. Larkin, C. Ho, and C.D. Stubbs, Lipids **31**, s189 (1996).
[29] B.J. Litman and D.C. Mitchell, Lipids **31**, s193 (1996).
[30] D.C. Mitchell and B.J. Litman, Biophys. J. **74**, 879 (1998).
[31] C.D. Niebylski and N. Salem, Jr., Biophys. J. **67**, 2387 (1994).
[32] A.C. Dumaual, L.J. Jenski, and W. Stillwell, Biochim. Biophys. Acta **1463**, 395 (2000).
[33] W. Rawicz, K.C. Olbrich, T. McIntosh, D. Needham, and E. Evans, Biophys. J. **79**, 328 (2000).
[34] R.W. Pastor, Curr. Opin. Struct. Biol. **4**, 486 (1994).
[35] K.V. Damodaran and K. M. Merz, Jr., in *Reviews in Computational Chemistry*, edited by K.B. Lipkowitz and D.B. Boyd (VCH, New York, 1994), Vol. 5, pp. 269–298.
[36] D.J. Tobias, K. Tu, and M.L. Klein, Curr. Opin. Colloid Interface Sci. **2**, 15 (1997).
[37] D.P. Tieleman, S.J. Marrink, and H.J.C. Berendsen, Biochim. Biophys. Acta, **1331**, 235 (1997).
[38] H. Heller, M. Schaefer, and K. Schulten, J. Phys. Chem. **97**, 8343 (1993).
[39] S.W. Chiu, E. Jakobsson, S. Subramaniam, and H.L. Scott, Biophys. J. **77**, 2462 (1999).
[40] K. Murzin, T. Rog, G. Jezierski, Y. Takaoka, and M. Pasenkiewicz-Gierula, Biophys. J. **81**, 170 (2001).
[41] M.A. Wilson and A. Pohorille, J. Am. Chem. Soc. **116**, 1490-(1994).
[42] P. Huang, J.j. Perez, and G.H. Loew, J. Biomol. Struct. Dyn. **11**, 927 (1994).
[43] S.E. Feller, D. Yin, R.W. Pastor, and A.D. Mackerell, Jr., Biophys. J. **73**, 2269 (1997).
[44] R.S. Armen, O.D. Uitto, and S.E. Feller, Biophys. J. **75**, 734 (1998).
[45] A.L. Rabinovich, P.O. Ripatti, and N.K. Balabaev, J. Biol. Phys. **25**, 245 (1999).
[46] A.L. Rabinovich, P.O. Ripatti, and N.K. Balabaev, Proc. SPIE **3687**, 175 (1999).
[47] A.L. Rabinovich, P.O. Ripatti, and N.K. Balabaev, Proc. SPIE **4064**, 144 (2000).
[48] A.L. Rabinovich, P.O. Ripatti, and N.K. Balabaev, Zh. Fiz. Khim., **74**, 1990 (2000) [Russ. J. Phys. Chem. **74**, 1809 (2000)].
[49] A.L. Rabinovich, P.O. Ripatti, and N.K. Balabaev, Proc. SPIE **4348**, 207 (2001).
[50] N.K. Balabaev, A.L. Rabinovich, P.O. Ripatti, and V.V. Kornilov, Proc. SPIE **3345**, 198 (1998).
[51] N.K. Balabaev, A.L. Rabinovich, P.O. Ripatti, and V.V. Kornilov, Zh. Fiz. Khim., **72**, 686 (1998) [Russ. J. Phys. Chem. **72**, 595 (1998)].
[52] A.L. Rabinovich and N.K. Balabaev, Proc. SPIE **4348**, 215 (2001).
[53] M.T. Hyvönen, M. Ala-Korpela, J. Vaara, T.T. Rantala, and J. Jokisaari, Chem. Phys. Lett. **246**, 300 (1995).
[54] M.T. Hyvönen, T.T. Rantala, and M. Ala-Korpela, Biophys. J. **73**, 2907 (1997).
[55] M.T. Hyvönen, M. Ala-Korpela, J. Vaara, T.T. Rantala, and J. Jokisaari, Chem. Phys. Lett. **268**, 55 (1997).
[56] L. Saiz and M.L. Klein, Biophys. J. **81**, 204 (2001).
[57] L.L. Pearce and S.C. Harvey, Biophys. J. **65**, 1084 (1993).
[58] Y.K. Levine, A. Kolinski, and J. Skolnick, J. Chem. Phys. **98**, 7581 (1993).
[59] U.A. van der Heide and Y.K. Levine, Biochim. Biophys. Acta, **1195**, 1 (1994).

[60] U.A. van der Heide and Y.K. Levine, Mol. Phys. **83**, 1251 (1994).
[61] Y.K. Levine, A. Kolinski, and J. Skolnick, J. Chem. Phys. **95**, 3826 (1991).
[62] A. Rey, A. Kolinski, J. Skolnick, and Y.K. Levine, J. Chem. Phys. **97**, 1240 (1992).
[63] Y.K. Levine, Mol. Phys. **78**, 619 (1993).
[64] N.K. Balabaev, A.L. Rabinovich, and P.O. Ripatti, Biofiz. **39**, 312 (1994) [Biophysics (Engl. Transl.) **39**, 283 (1994)].
[65] M.R. Rich, Biochim. Biophys. Acta **1178**, 87 (1993).
[66] V.G. Dashevskii and A.L. Rabinovich, Vysokomol. Soedin. Ser. A **25**, 544 (1983) [Polym. Sci. U.S.S.R. **25**, 638 (1983)].
[67] A.L. Rabinovich, Makromol. Chem. **192**, 359 (1991).
[68] A.L. Rabinovich, P.O. Ripatti, and V.G. Dashevskii, Biofiz. **30**, 802 (1985) [Polym. Sci. U.S.S.R. **30**, 871 (1985)].
[69] A.L. Rabinovich, V.G. Dashevskii, and P.O. Ripatti, Vysokomol. Soedin., Ser. A **28**, 1697 (1986) [Polym. Sci. U.S.S.R. **28**, 1891 (1986)].
[70] A.L. Rabinovich and P.O. Ripatti, Proc. SPIE **4348**, 225 (2001).
[71] A.L. Rabinovich and P.O. Ripatti, Dokl. Akad. Nauk (SSSR) **314**, 752 (1990).
[72] A.L. Rabinovich and P.O. Ripatti, Biochim. Biophys. Acta **1085**, 53 (1991).
[73] A.L. Rabinovich and P.O. Ripatti, Biofiz. **35**, 775 (1990) [Biophysics (Engl. Transl.) **35**, 803 (1990)].
[74] A.L. Rabinovich and P.O. Ripatti, Chem. Phys. Lipids **58**, 185 (1991).
[75] A.L. Rabinovich and P.O. Ripatti, Biofiz. **40**, 1214 (1995) [Biophysics (Engl. Transl.) **40**, 1227 (1995)].
[76] A.L. Rabinovich and P.O. Ripatti, Biofiz. **41**, 1221 (1996) [Biophysics (Engl. Transl.) **41**, 1241 (1996)].
[77] A.L. Rabinovich and P.O. Ripatti, Proc. SPIE **3345**, 193 (1998).
[78] A.L. Rabinovich and P.O. Ripatti, Zh. Fiz. Khim. **72**, 681 (1998) [Russ. J. Phys. Chem. **72**, 590 (1998)].
[79] A.L. Rabinovich and P.O. Ripatti, Dokl. Akad. Nauk **364**, 264 (1999) [Phys. Dokl. **364**, 6 (1999)].
[80] A.L. Rabinovich and P.O. Ripatti, Biol. Membrany **16**, 563 (1999) [Membr Cell Biol. **13**, 697 (2000)].
[81] K.R. Applegate and J.A. Glomset, J. Lipid Res. **27**, 658 (1986).
[82] K.R. Applegate and J.A. Glomset, J. Lipid Res. **32**, 1635 (1991).
[83] K.R. Applegate and J.A. Glomset, J. Lipid Res. **32**, 1645 (1991).
[84] S. Li, H.-N. Lin, Z.-Q. Wang, and C. Huang, Biophys. J. **66**, 2005 (1994).
[85] S. Li and C. Huang, J. Comput. Chem. **17**, 1013 (1996).
[86] F.A.M. Leermakers and J.M.H.M. Scheutjens, J. Chem. Phys., **89**, 3264 (1988).
[87] F.A.M. Leermakers and J.M.H.M. Scheutjens, J. Chem. Phys., **103**, 10332 (1995).
[88] F.A.M. Leermakers and J.M.H.M. Scheutjens, J. Chem. Phys. **89**, 6912 (1988).
[89] F.A.M. Leermakers, J.M.H.M. Scheutjens, and J. Lyklema, Biochim. Biophys. Acta **1024**, 139 (1990).
[90] F.A.M. Leermakers and J.M.H.M. Scheutjens, J. Colloid Interface Sci. **136**, 231 (1990).
[91] D.R. Fattal and A. Ben-Shaul, Biophys. J. **67**, 983 (1994).
[92] L.G. Abood, N. Salem, Jr., M. MacNeil, L. Bloom, and M.E. Abood, Biochim. Biophys. Acta **468**, 51 (1977).
[93] L.G. Abood, N. Salem, Jr., M. MacNeil, and M. Batler, Biochim. Biophys. Acta **530**, 35 (1978).
[94] J. Ernst, W.S. Sheldrick, and J.-H. Fuhrhop, Z. Naturforsch. B **34**, 706 (1979).
[95] W.L. Jorgensen, J. Chandrasekar, J.D. Madura, R.W. Impey, and M.L. Klein, J. Chem. Phys. **79**, 926 (1983).
[96] W.D. Cornell, P. Cieplak, C.L. Bayly, I.R. Gould, K.M. Merz, Jr., D.M. Ferguson, D.C. Spellmeyer, T. Fox, J.W. Caldwell, and P.A. Kollman, J. Am. Chem. Soc. **117**, 5179 (1995).
[97] J.E. Baenziger, H.C. Jarrell, R.J. Hill, and I.C.P. Smith, Biochemistry **30**, 894 (1991).
[98] J.-P. Jøstensen, Dr. Sci. thesis, Tromsø, Norway, 1998.
[99] T.R. Stouch, K.B. Ward, A. Altieri, and A.T. Hagler, J. Comput. Chem. **12**, 1033 (1991).
[100] P.J. Flory, *Statistical Mechanics of Chain Molecules* (Interscience, New York, 1969).
[101] V.G. Dashevskii, *Conformational Analysis of Organic Molecules* (in Russian) (Nauka, Moscow, 1982).
[102] M. Schlenkrich, J. Brickmann, A. D. MacKerell, Jr., and M. Karplus, in *Biological Membranes*, edited by K. Merz, Jr. and B. Roux (Birkhauser, Boston, 1996), pp. 31–81.
[103] M.P. Allen and D.J. Tildesley, *Computer Simulation of Liquids* (Clarendon Press, Oxford, 1987).
[104] R.J. Sadus, *Molecular Simulations of Fluids. Theory, Algorithms and Object-Orientation* (Elsevier, Amsterdam, 1999).
[105] N.K. Balabaev and A.A. Lemak, Mol. Simul. **15**, 223 (1995).
[106] R. Koynova and M. Caffrey, Biochim. Biophys. Acta **1376**, 91 (1998).
[107] G.J. Fleer, M.A. Cohen Stuart, J.M.H.M. Scheutjens, T. Cosgrove, and B. Vincent, *Polymers at Interfaces* (Chapman and Hall, London, 1993).
[108] F.A.M. Leermakers, J.M.H.M. Scheutjens, and J. Lyklema, Biophys. Chem. **18**, 353 (1983).
[109] F.A.M. Leermakers, A.L. Rabinovich, and N.K. Balabaev, Phys. Rev. E. **67**, 011910 (2003).
[110] L.A. Meijer, F.A.M. Leermakers, and J. Lyklema, J. Chem. Phys. **110**, 6560 (1999).
[111] L.A. Meijer, F.A.M. Leermakers, and J. Lyklema, Recl. Trav. Chim. Pays-Bas. **113**, 167 (1994).
[112] S.M. Oversteegen, P.A. Barneveld, J. van Male, F.A.M. Leermakers, and J. Lyklema, Phys. Chem. Chem. Phys. **1**, 4987 (1999).
[113] S.M. Oversteegen and F.A.M. Leermakers, Phys. Rev. E **62**, 8453 (2000).
[114] J. Seelig and N. Waespe-Šarčević, Biochemistry **17**, 3310 (1978).
[115] T. Huber, K. Rajamoorthi, V.F. Kurze, K. Beyer, and M.L. Brown, J. Am. Chem. Soc. **124**, 298 (2002).
[116] S.E. Feller, K. Gawrisch, and A.D. MacKerell, Jr., J. Am. Chem. Soc. **124**, 318 (2002).
[117] A.L. Rabinovich, P.O. Ripatti, N.K. Balabaev, and F.A.M. Leermakers, Proc. SPIE **4627**, 141 (2002).